FINAL REPORT
Prepared for Christmas Tree Promotion Board
June 2023

CTPB Project Number: 21-02-DU

Project Title: Mapping Christmas tree nutrition requirements using unmanned aerial vehicles and multispectral sensors

Principal Investigator: Dr. Mason MacDonald

Institution: Dalhousie University

TECHNICAL REPORT

Introduction

Christmas tree fertilization is necessary to maintain tree growth, color, pest resistance, and needle retention. Nitrogen is the nutrient most likely to be lacking for Christmas tree growth and color development (Hart et al., 2009; Lamontagne et al., 2019). Needle nitrogen concentrations of between 1.4% and 1.6% are adequate for growth, though higher concentrations are beneficial for color and needle retention (Hart et al., 2009; MacDonald et al., 2018). Fertilization is recommended either once or twice per year. The most critical time of year to apply fertilizer is in spring, typically between mid-April and mid-June. If a second application of fertilizer is needed, then it would typically be applied in late-June or July (HD4212, n.d.). Traditionally, fertilizers are applied to soils under the tree drip line by hand, though motorized and aerial application may also be used depending on the size of the field (Hart et al. 2009).

There are many challenges facing the environmental sustainability of Christmas tree fertilization. First, Christmas trees only incorporated 21% of applied nitrogen with 30% remaining in the soil. The remaining 49% is lost primarily through leaching and denitrification, with each posing significant environmental risks (Hart et al., 2009). Second, tissue sampling is typically recommended over soil sampling because trees are slower to respond to nutrient changes than other agricultural species (Spectrum Analytic, n.d.). Needle tissue should be sampled to ensure nutrient concentrations remain within an acceptable range because changes due to fertilization may not be observed until the following season (Hart et al., 2009). Third, nutrient concentration in both soil and plant tissue are highly variable by sampling location and season (MacDonald et al., 2018). An improved method of detecting Christmas tree nutrient requirements is needed.

Remote sensing is the process of obtaining information about objects using specific wavelengths of electromagnetic radiation and has exhibited considerable potential in the quantitative determination of plant nutrition (Liu et al. 2017). Several different indices have been developed to estimate nutrition, often using a combination of visible and near infra-red wavelengths (Wojtowicz et al., 2016). Remote sensing to evaluate plant nutrition offers several advantages over other methods, such as ease of use, decreased time for analysis, non-destructive sampling, the ability to analyze large areas, and working in tandem with other precision agriculture technologies (e.g. variable rate application). The use of remote sensing in Christmas trees would allow producers to quickly ascertain individual tree fertilizer needs, thus decreasing cost and environmental impact.

The purpose of this proposed to study would be to evaluate whether remote sensing could accurately detect differences in Christmas tree foliar nutrient concentrations. It is hypothesized that remote sensing could estimate foliar nutrition. If the hypothesis is correct, then a predictive model for foliar nitrogen could be developed from multispectral data.

Methods

Site Description

Two balsam fir orchards were chosen to collect samples in autumn 2021: one on Belmont Road, Belmont, NS (45.43N, 63.38W) and one on College Road, Bible Hill, NS (45.37N, 63.24W) (Fig.1). All trees were tagged and then 25 were randomly selected from each location for analysis in November 2022. The specific GPS coordinates of all 50 sampled trees were recorded.

A second round of sampling was conducted in spring 2022 prior to any fertilization with a third orchard added to increase the number of samples. The third orchard was also located at the same site on College Road, slightly southeast of the orchard sampled in autumn 2021. An additional 25 trees were tagged in the new orchard to increase the sample size to 75 trees.

Figure 1. Satellite image of sample sites where the red B represents Belmont Road, Belmont, NS and the yellow C represents College Road, Bible Hill, NS. There was one orchard used from each site in autumn 2021. There was one orchard from Belmont Road and two orchards from College Road in spring 2022.

Nutrient Analysis

Six soil samples were collected from around the dripline of each tree and homogenized into a single representative sample. Soil was oven dried, ground with mortar and pestle, and sieved through a 2 mm stainless steel sieve. The Mehlich 3 soil extractant was used to obtain the plant available nutrients in the soil. Ten grams of moist soil was placed in a plastic container with 100 mL of Mehlich 3 and shaken for 15 minutes at 200 oscillations per minute. The supernatant was filtered through Whitman No. 5 paper and analyzed using a Jarell-Ash Inductively Coupled Argon Plasma Emissions Spectrometer (ICAP).

Two branches were cut from each tree at the most recent 2 years growth. Needles were removed from the branches, dried, and then ground through a 1 mm steel screen. One gram needle tissue was placed in a 250 mL digestion tube with 15 mL of nitric acid. Samples were placed on a digestion block at 90°C for 45 minutes and then the temperature was increased to 140°C until it was clear and approximately 1 mL was remaining. Nitric acid (1%) was added and the samples were filtered and put into a volumetric flask. Total N was measured using a LECO model FP 528 analyzer. Analysis of P, K, Ca, Mg, S, Fe, Zn, Mn, B, and Cu was conducted with inductively coupled plasma atomic emission spectroscopy (ICP-OES).

Aerial Image Acquisition and Equipment

On June 2nd, 2022, aerial images were captured over each Christmas tree field using a DJI M300 RTK drone (SZ DJI Technology Co., Ltd., Shenzhen, China). This drone was equipped with a Micasense Altum multispectral camera (MicaSense, Inc., Seattle, WA, USA) capable of recording imagery across five distinct spectral ranges. The spectral bands encompassed blue (Band 1-459-491 nm), green (Band 2 - 546-573 nm), red (Band 3-661–675 nm), red-edge (Band 4-710–723 nm), and near-infrared (Band 5-813–870 nm)(MicaSense, 2023).

Flight and Survey Parameters

Utilizing the DJI Pilot app (SZ DJI Technology Co., Ltd., Shenzhen, China), the surveys were systematically planned and executed at an altitude of 90 meters above ground level (AGL). The flight parameters were established to ensure a 75% overlap in both forward and lateral directions. The camera was set at nadir (90°) orientation, and the flight path was configured as a single grid.

Positioning Accuracy and Ground Control Points

A D-RTK2 base station (SZ DJI Technology Co., Ltd., Shenzhen, China) was deployed during the surveys to minimize the positional inaccuracies in the acquired images. Ground control points (GCPs) were also placed evenly across the survey areas to enhance post-processing accuracy. Six and nine GCPs were implemented across Sites 1 (College Road) and 2 (Belmont), respectively. The coordinates of these GCPs were precisely recorded with an Emlid Reach RS2 multi-frequency Global Navigation Satellite System (GNSS) receiver (Emlid Inc., Hong Kong, China) set in survey mode and connected to a networked transport of RTCM via internet protocol (NTRIP) correction service.

Image Processing, Camera Calibration and Reflectance Correction

The collected multispectral images underwent a processing sequence in Agisoft PhotoScan 2.0.2 (Agisoft LLC Inc., St. Petersburg, Russia) to yield an orthomosaic representation of the study areas. The Altum camera was calibrated using a Calibrated Reflectance Panel (CPR) to compensate for incident light conditions. The CPR calibration is vital for maintaining the precision of the subsequent image analysis and comparing values between two surveys as it assigns a definitive reflectance value during the corrections process. The surface values of the CPR were predetermined with a spectrometer at several wavelengths and provided by MicaSense (MicaSense, 2023). Images of the CPR were taken before and after each flight, and the reflectance was calibrated in the processing stages in Agisoft (Agisoft LLC, 2023).

Image Interpretation and Noise Reduction

The Percent clip stretch type was selected during image interpretation to help visualize the orthomosaic and distinguish ground features from Christmas trees. This stretch function enhanced the orthomosaic by applying a linear stretch between the highest and lowest pixel values, translating into a more precise Christmas tree representation. The orthomosaic was then purged of elements beyond the study areas to augment the classification accuracy and minimize extraneous noise. This process is considered necessary as features such as houses, roads, and cars often constitute unwanted pixel values and pose challenges during the optimization parameters of the image classification (Pal & Mather, 2005).

Supervised Image Classification
Subsequently, a supervised image classification was performed using the Support Vector Machine (SVM) classifier. This technique facilitated the classification of pixels with similar values within the multispectral orthomosaic. The SVM classifier was selected due to its low sample requirement and robustness against noise and correlated bands (ESRI, 2023b; Pal & Mather, 2005). Training samples were collected and managed using the Training Samples Manager in ArcGIS Pro, classifying images into four categories: Christmas Tree, Shadows, Bare ground, and Grass. Fifty samples per class were collected to train the classifier, resulting in 200 training samples for each study site.

Normalized Difference Vegetation Index Calculation and Interpretation
The Normalized Difference Vegetation Index (NDVI) is a standardized index utilized to generate an image quantifying vegetation greenness (ESRI, 2023a). The NDVI index leverages the contrast between the characteristics and chlorophyll pigment absorption of the Red and Near-infrared bands (Xue & Su, 2017). The following formula was used to compute the NDVI, utilizing the Band 3 and Band 4 of the Altum multispectral camera:

$$NDVI=((NIR-Red))/((NIR+Red)) \quad (1)$$

Areas with low NDVI values corresponded to areas with sparse or no vegetation, such as rock or bare soil. Moderate values indicate shrubs and grassland, while high values denote forested areas and lush vegetation (Antognelli, 2018; ESRI, 2023a).

Feature Extraction and Outlier Removal
Following the creation of the NDVI maps, all features classified as Christmas trees from the classified raster were extracted and overlayed on the NDVI maps, which allowed the extraction of NDVI pixel values for each Christmas tree. Using the zonal statistics tool in ArcGIS Pro, the mean pixel values within each Christmas Tree polygon were calculated. This allowed the computation of the mean pixel value for each Christmas Tree, which was then used to compare NDVI values from one tree to another.

Statistical Analysis
All statistical analysis was completed using Minitab 19 software. Soil and tissue nutrition were compared between sites using an analysis of variance. Correlation analysis was used to try and identify significant relationships between soil and tissue nutrition and balsam fir NDVI. Balsam trees were classified as younger than 5 years and older than 5 years and the correlation analysis was repeated. The most significant correlations were submitted to a linear regression analysis.

Results and Discussion

Soil and Tissue Nutrition
The two sites had significantly different soil nutrient profiles in Autumn 2021. Belmont Road had significantly higher soil concentrations of N, K, and Zn while College Road (Site 1) had significantly higher concentrations of P, Cu, and Mn Table 1). There were no significant differences between other six measured minerals (i.e. Ca, Mg, Na, S, Al, and Fe). Soil nutrition profiles had similar trends in Spring 2022 with respect to Belmont and College Road (Site 1). College Road (Site 2) generally had comparable nutrient concentrations to College Road (Site 2), with the exception that Site 2 had significantly more K and less Cu than Site 1 (Table 2). Differences in soil nutrition between sites were expected, since the site in Belmont is an actively managed commercial lot while the lot in Bible Hill is a research site with limited soil management.

The two sites had significant differences in needle tissue profiles in Autumn 2021. Belmont Road had significantly higher needle tissue concentrations of N, while College Road (Site 1) had significantly higher concentrations of Ca and Mn (Table 3). There were no significant differences between all other measured minerals (i.e. P, K, Mg, Na, B, Fe, and Zn). Belmont Road had significantly higher needle concentration of N in Spring 2022, but lower K, Ca, and Mn. Belmont Road had lower Fe than College Road (Site 1) but higher Fe than College Road (Site 2). As above, it was expected that the Belmont field would have higher N due to repeated fertilizer application at that site compared to Bible Hill. It was expected that P would also be significantly higher in Belmont, but the soil concentration of P was only 2 times as high as Bible Hill while the concentration of N was 10 times higher.

The concentration of soil nutrients and needle tissue nutrients were not significantly related in most cases, except for N and Mn. Both N and Mn had significant ($P < 0.01$) positive relationships between soil and needle tissues (Fig. 2). Soil N accounted for 23% of variation in tissue N and soil Mn accounted for 61% of variation in tissue N. It must be noted that the R^2 value for Mn was inflated slightly due to the presence of 2 influential points at approximately 100ppm and 150 ppm in soil. However, the relationship remains statistically significant even without these two points.

Table 1. Soil nutrition of two Nova Scotian balsam fir orchards (along Belmont Road, Belmont, NS and College Road, Bible Hill, NS) in Autumn 2021. Data expressed as mean ± standard error as calculated from 25 replicates in each site. Boron was below the detectable limit so not shown on the table.

Nutrient	**Belmont**			**College (Site 1)**		
N (ppm)	13.81	±	1.38	7.24	±	0.71
P (kg/ha)	360.86	±	33.37	576.88	±	28.28
K (kg/ha)	248.19	±	19.58	130.52	±	7.25
Ca (kg/ha)	1960.95	±	88.80	2070.92	±	71.66
Mg (kg/ha)	363.57	±	25.57	330.04	±	13.26
Na (kg/ha)	54.62	±	22.09	29.44	±	1.32
S (kg/ha)	24.86	±	0.54	23.60	±	0.59
Al (ppm)	1421.14	±	20.24	1399.52	±	24.20
Cu (ppm)	1.18	±	0.04	2.00	±	0.15
Fe (ppm)	142.10	±	6.77	137.72	±	6.67
Mn (ppm)	31.67	±	1.54	54.88	±	4.52
Zn (ppm)	3.09	±	0.19	1.05	±	0.06

Table 2. Soil nutrition of three Nova Scotian balsam fir orchards (along Belmont Road, Belmont, NS and College Road, Bible Hill, NS) in Spring 2022. Data expressed as mean ± standard error as calculated from 25 replicates in each site. Boron was below the detectable limit so not shown on the table.

Nutrient	Belmont			College (Site 1)			College (Site 2)		
N (ppm)	31.10	±	3.66	1.99	±	0.22	2.11	±	0.14
P (kg/ha)	397.92	±	34.15	611.68	±	24.82	626.76	±	23.20
K (kg/ha)	359.96	±	34.86	166.04	±	10.97	334.36	±	17.70
Ca (kg/ha)	2190.64	±	93.81	2264.68	±	73.78	1959.68	±	56.03
Mg (kg/ha)	381.00	±	26.61	355.88	±	16.77	349.08	±	14.50
Na (kg/ha)	71.16	±	24.00	34.44	±	1.29	32.92	±	1.60
S (kg/ha)	34.60	±	1.21	29.36	±	0.55	28.16	±	0.50
Al (ppm)	1538.08	±	20.13	1429.24	±	28.66	1537.00	±	21.77
Cu (ppm)	1.26	±	0.04	2.09	±	0.14	1.30	±	0.16
Fe (ppm)	136.92	±	6.15	147.52	±	7.51	143.48	±	5.07
Mn (ppm)	32.72	±	1.61	68.32	±	5.74	61.36	±	2.15
Zn (ppm)	3.63	±	0.19	1.99	±	0.22	2.11	±	0.14

Table 3. Needle tissue nutrition of two Nova Scotian balsam fir orchards (along Belmont Road, Belmont, NS and College Road, Bible Hill, NS) in Autumn 2021. Data expressed as mean ± standard error as calculated from 25 replicates in each site. Copper was below the detectable limit so not shown on the table.

Nutrient	Belmont			College (Site 1)		
N (%)	1.75	±	0.06	1.32	±	0.05
P (%)	0.20	±	0.01	0.17	±	0.01
K (%)	0.53	±	0.02	0.47	±	0.02
Ca (%)	0.68	±	0.05	1.13	±	0.06
Mg (%)	0.09	±	0.00	0.10	±	0.00
Na (%)	0.02	±	0.00	0.02	±	0.00
B (ppm)	18.62	±	1.23	15.75	±	1.19
Fe (ppm)	43.67	±	2.72	44.95	±	2.85
Mn (ppm)	238.05	±	30.33	694.79	±	82.24
Zn (ppm)	45.87	±	3.49	54.48	±	3.57

Table 4. Needle tissue nutrition of three Nova Scotian balsam fir orchards (along Belmont Road, Belmont, NS and College Road, Bible Hill, NS) in Spring 2022. Data expressed as mean ± standard error as calculated from 25 replicates in each site. Copper and sodium were below the detectable limit so not shown on the table.

Nutrient	Belmont			College (Site 1)			College (Site 2)		
N (%)	1.31	±	0.04	1.17	±	0.03	1.11	±	0.03
P (%)	0.12	±	0.01	0.13	±	0.01	0.13	±	0.01
K (%)	0.31	±	0.01	0.44	±	0.02	0.44	±	0.01
Ca (%)	0.74	±	0.05	1.00	±	0.05	1.08	±	0.03
Mg (%)	0.07	±	0.01	0.08	±	0.01	0.10	±	0.01
B (ppm)	14.62	±	0.85	15.76	±	1.07	14.37	±	0.68
Fe (ppm)	58.96	±	3.70	127.50	±	26.8	37.48	±	7.10
Mn (ppm)	283.2	±	31.64	666.91	±	70.03	602.00	±	45.50
Zn (ppm)	44.89	±	3.37	48.40	±	3.08	41.36	±	2.84

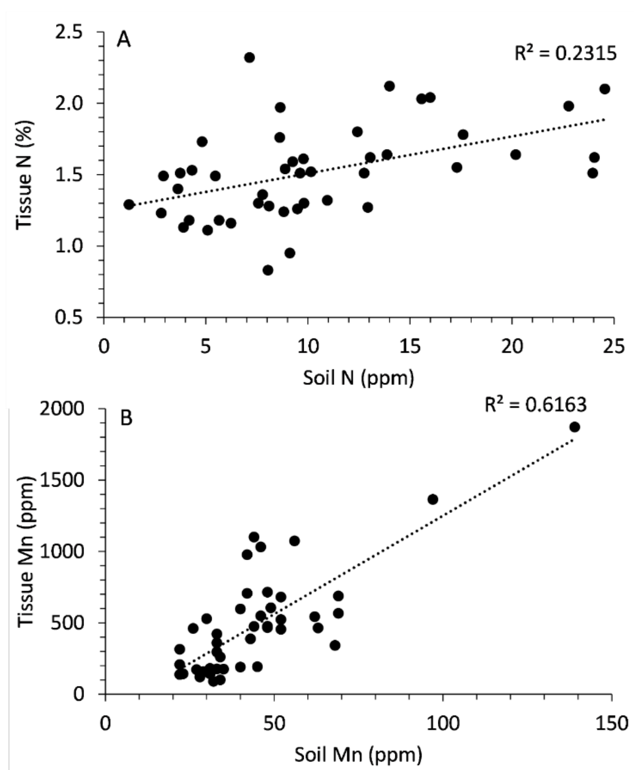

Figure 2. Significant (P < 0.01) relationships between A) soil N and needle tissue N and, B) soil Mn and needle tissue Mn. N =50 in each graph.

NDVI and Nutrition

NDVI maps were created for each site (Fig. 3 and Fig. 4). The average NDVI for balsam trees was about 0.65 and ranged from approximately 0.50 to 0.80. However, the 95% confidence interval was 0.692 ± 0.011 in autumn and 0.684 ± 0.010 in spring. There was very low variability in balsam fir NDVI in general.

There were only weak correlations between soil nutrition and overall NDVI (Table 5). However, there were some significant correlations after younger trees were separated from older trees in the analysis. In both autumn and spring, NDVI of trees < 5 years old was positively correlated with Na and Mn Table 5). NDVI was also negatively correlated with autumn S and spring K in trees > 5 years old (Table 5).

There were several significant correlations between foliar nutrition and overall NDVI (Table 6). N, P, K were all positively correlated with NDVI in autumn (Table 6). However, these correlations were all stronger in trees > 5 years old. Of those three nutrients, only N and P were correlated with NDVI in both autumn and spring. N was of particular interest because the coefficient of determination (R^2) was relatively high in younger trees, with NDVI explaining approximately 60% and 50% of variability in tissue N of trees in autumn and spring, respectively.

There are many studies detailing remote sensing metrics in annual crops, including NDVI. However, it has been notably more difficult to determine relationships between spectral and growth characteristics in tree species (Atzberger 2013). Among other issues, trees crops are in production for many years such that tree age could be an important factor. Age has a significant effect on vegetation indices due to the changes in canopy coverage, soil effects, physiology, and other factors (McMorrow 2001; Moreira 2004, Chemura et al. 2017). Age appears to be a major factor in NDVI is balsam fir as well, where NDVI is a better indicator of foliar nutrition in trees older than 5 years.

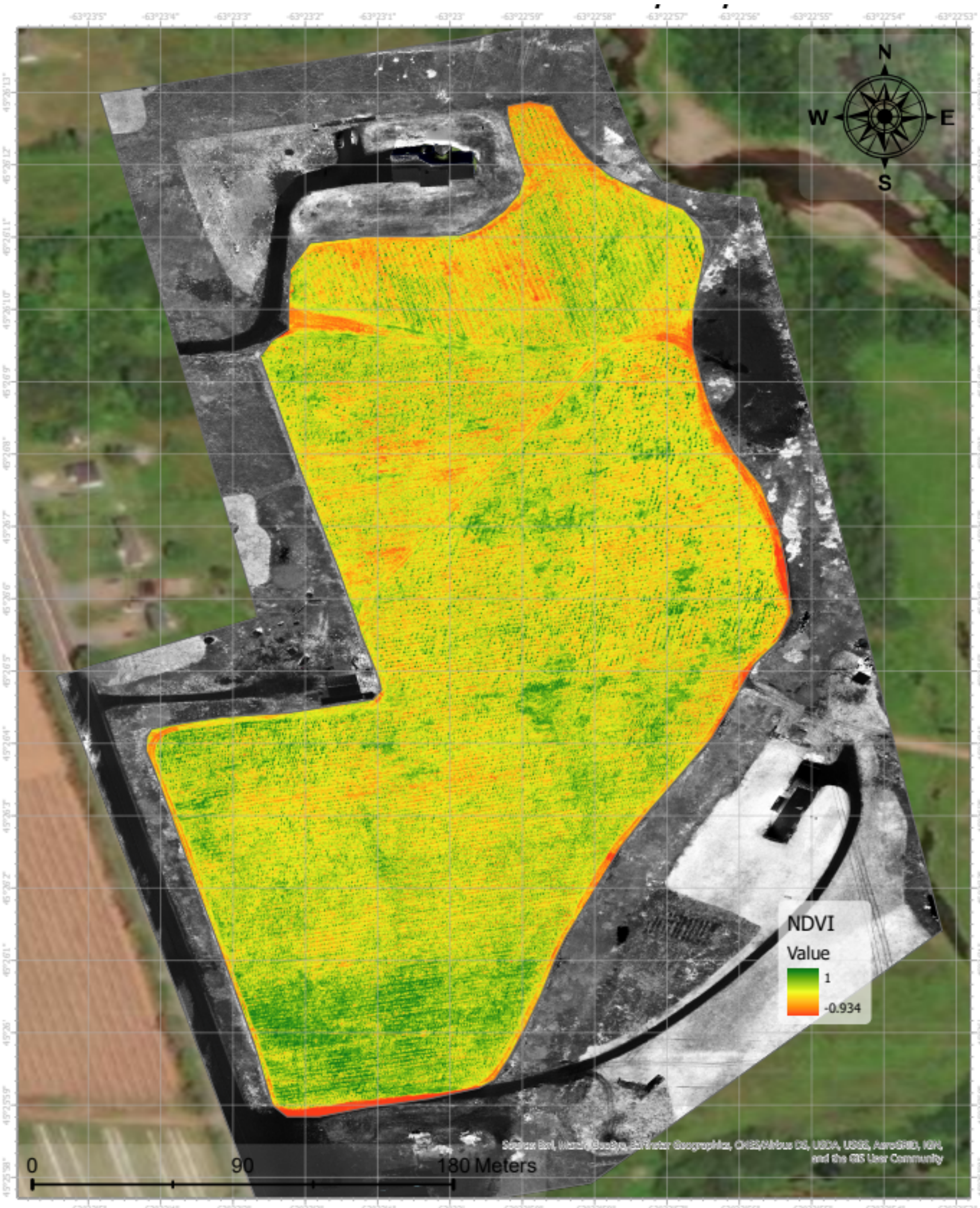

Figure 3. Normalized difference vegetation index of balsam fir orchard on Belmont Road, Belmont, NS.

Figure 4. Normalized difference vegetation index of balsam fir orchard on College Road, Bible Hill, NS.

Table 5. Correlation coefficients of autumn and spring soil nutrition with NDVI. Correlations are shown for all trees and then separated into trees less than and greater than 5 years old.

Nutrient	Autumn 2021			Spring 2022		
	Overall	< 5 year	>5 year	Overall	< 5 year	>5 year
N	-0.13	-0.28	0.23	0.02	-0.08	0.02
P	0.00	0.06	0.11	-0.10	-0.09	-0.14
K	0.18	0.15	0.20	-0.26	-0.13	-0.35
Ca	0.01	-0.21	0.26	0.12	-0.12	0.26
Mg	0.00	-0.15	0.21	0.06	-0.11	0.19
Na	0.33	0.43	0.04	0.28	0.50	0.19
S	-0.16	0.20	-0.49	0.04	0.07	0.01
Al	-0.14	0.02	-0.28	-0.11	-0.04	-0.15
Cu	-0.13	0.24	-0.20	0.04	0.21	0.03
Fe	0.17	0.15	0.19	0.07	0.22	0.01
Mn	0.05	0.53	0.05	0.03	0.36	0.02
Zn	0.04	-0.20	0.14	-0.07	-0.03	-0.26

Table 6. Correlation coefficients of autumn and spring foliar nutrition with NDVI. Correlations are shown for all trees and then separated into trees less than and greater than 5 years old.

Nutrient	Autumn 2021			Spring 2022		
	Overall	< 5 year	>5 year	Overall	< 5 year	>5 year
N	0.55	0.48	0.78	0.55	0.30	0.67
P	0.45	0.35	0.47	0.30	0.10	0.36
K	0.52	0.36	0.60	0.07	0.02	0.13
Ca	-0.04	-0.09	0.11	0.16	0.19	0.24
Mg	-0.04	-0.31	0.29	-0.11	0.00	-0.15
Na	0.30	0.32	0.32	n/a	n/a	n/a
B	0.08	-0.03	0.17	-0.08	-0.47	0.03
Fe	-0.07	-0.03	-0.10	0.13	0.15	0.15
Mn	-0.05	0.06	0.00	0.19	0.34	0.23
Zn	0.30	0.37	0.23	0.48	0.49	0.49

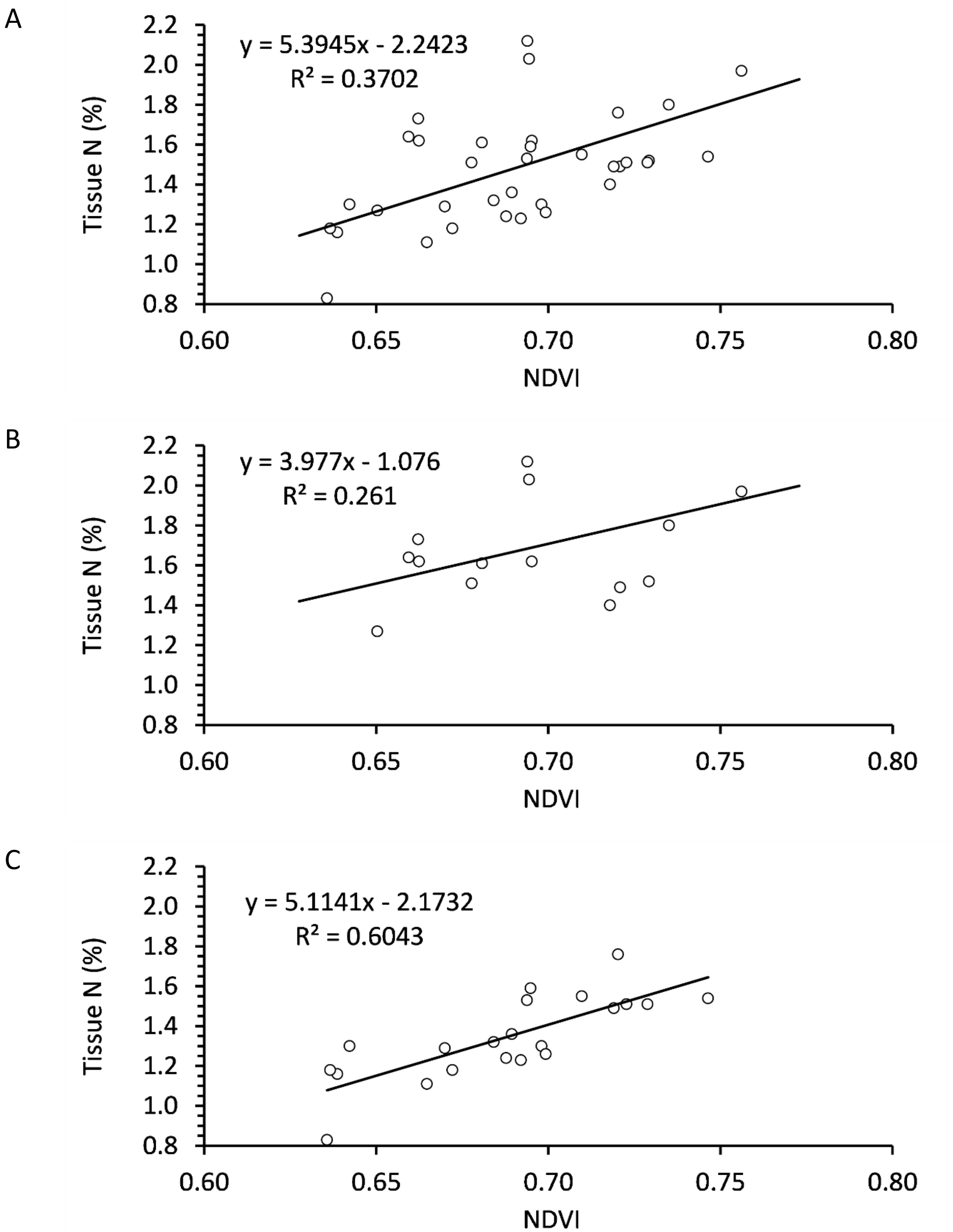

Table 7. Relationship of NDVI and tissue N in autumn for A) all trees (N = 50), B) trees < 5 years old (N -25), and C) trees > 5 years old (N = 25).

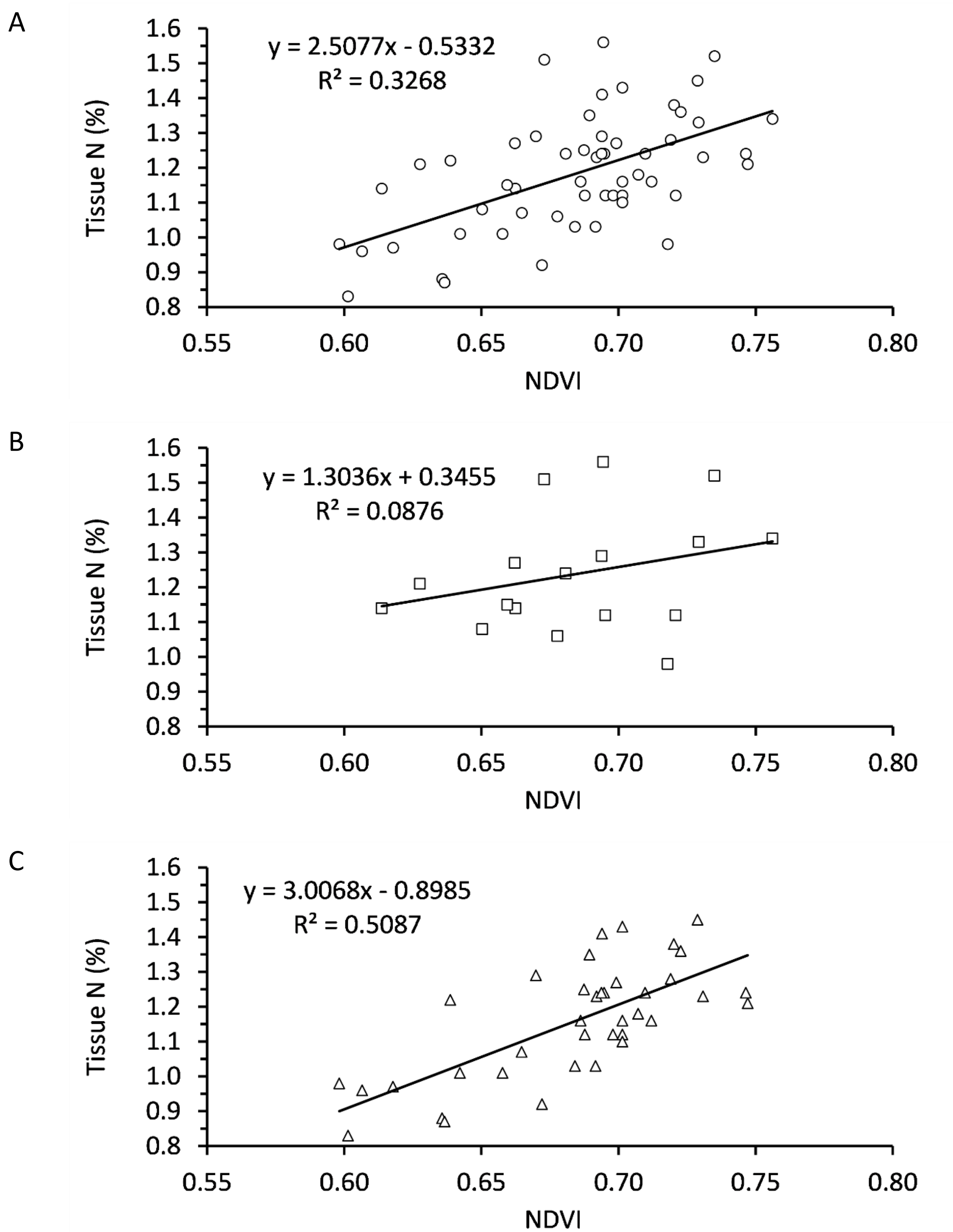

Table 8. Relationship of NDVI and tissue N in spring for A) all trees (N = 50), B) trees < 5 years old (N -25), and C) trees > 5 years old (N = 25).

Conclusion and Recommendations

Mapping NDVI can be a useful predictive tool to estimate tissue N in more mature balsam fir trees (> 5 years old), but any predictive power is decreased for younger trees or mixed age stands. NDVI explained 60% of tissue N variability in autumn and 50% of tissue N variability in spring. It is recommended that this study be extended to include a higher number of balsam fir stands to further explore the predictive power of NDVI for balsam, including stands outside of NS.

The biggest challenge interpreting NDVI maps was found in shadows cast by the trees. Our method cut away trees from shadows on the map to isolate NDVI values, which was more time intensive. Timing drone flights when sun is directly overhead and/or on days expected to have high cloud cover would greatly reduce complications caused by shadows.

References

Agisoft LLC. (2023). MicaSense Altum processing workflow (including Reflectance Calibration) in Agisoft Metashape Professional. Helpdesk Portal. https://agisoft.freshdesk.com/support/solutions/articles/31000148381-micasense-altum-processing-workflow-including-reflectance-calibration-in-agisoft-metashape-professi

Antognelli, S. (2018, May 28). NDVI and NDMI vegetation indices: Instructions for use. Agricolus. https://www.agricolus.com/en/vegetation-indices-ndvi-ndmi/

Atzberger C. 2013. Advances in remote sensing of agriculture: context description: existing operational monitoring systems and major information needs. Remote Sensing. 5: 949-981.

Chemura A, Mutanga O, Dube T. 2017. Integrating age in the detection and mapping of incongruous patches in coffee (*Coffea arabica*) plantations using multi-temporal Landsat 8 NDVI anomalies. Internation Journal of Applied Earth Observation and Geoinformation. 57: 1-13.

ESRI. (2023a). NDVI function, ArcGIS Pro documentation. https://pro.arcgis.com/en/pro-app/3.0/help/analysis/raster-functions/ndvi-function.htm

ESRI. (2023b). Train Support Vector Machine Classifier (Spatial Analyst), ArcGIS Pro documentation. https://pro.arcgis.com/en/pro-app/latest/tool-reference/spatial-analyst/train-support-vector-machine-classifier.htm

Hart J, Landgren C, Fletcher R, Bondi M, Withrow-Robinson B, Chastagner G. 2009. Christmas tree nutrient management guide. Oregon State University, Oregon, USA. pp. 62.

HD2412. n.d. Fertilization of Christmas trees. Accessed May 11, 2021 at https:// www.hd2412.co.uk/fertilization-of-christmas-trees.

Lamontagne M, Adegbidi HG, Assamoi AJ. 2019. Organic fertilization of Christmas tree (Abies balsamea (L.) Mill.) plantations with poultry manure in northwestern New Brunswick, Canada. The Forestry Chronicle. 95:39-49.

Liu H, Zhu, H, Wang P. 2017. Quantitative modelling for leaf nitrogen content of winter wheat using UAV-based hyperspectral data. International Journal of Remote Sensing. 38:2117-2134.

MacDonald MT, Lada RR. 2018. Seasonal changes in soil and tissue nutrition in balsam fir and influences on postharvest needle abscission. Scandinavian Journal of Forest Research. 33:426-436.

McMorrow J. 2001. Linear regression modeling for the estimation of oil palm age from landsat T<. Internation Journal of Remote Sensing. 22: 2243-2264.

MicaSense. (2023, January 6). User Guide for MicaSense Sensors. MicaSense Knowledge Base. https://support.micasense.com/hc/en-us/articles/360039671254-User-Guide-for-MicaSense-Sensors

Pal M, Mather PM. 2005/ Support vector machines for classification in remote sensing. International Journal of Remote Sensing, 26: 1007–1011. https://doi.org/10.1080/01431160512331314083

Spectrum Analytic Inc. n.d. Fertilizing Christmas trees. Spectrum Analytic Publishing. Washington, Ohio, USA. pp. 23.

Wojtowicz M, Wojtowics A, Piekarczyk J. 2016. Application of remote sensing methods in agriculture. Communications in Biometry and Crop Science. 11:31-50.

Xue J, Su B. 2017. Significant Remote Sensing Vegetation Indices: A Review of Developments and Applications [Research article]. Journal of Sensors. https://doi.org/10.1155/2017/1353691

EXECUTIVE SUMMARY OF RESEARCH REPORT (FOR PUBLIC RELEASE)

Two balsam fir fields were selected for this study: one in Belmont, NS (45.37N, 63.24W) and one in Bible Hill, NS (45.37N, 63.24W). All trees were tagged for identification and then 25 trees were randomly sampled from each field. Soil samples were taken along the dripline of each tree and two small branches were cut to obtain needle tissue samples. Simultaneously, an unmanned aerial vehicle equipped with a multi-spectral camera was flown over each site to collect imaging data. This was conducted once in autumn of 2021 and then again in spring 2022 with an additional 25 data points.

The two fields have several significant differences in soil and tissue nutrition. Perhaps most relevant is the fact that nitrogen concentrations are significantly higher in soils and tissues at the Belmont site. Higher nitrogen in Belmont is not unexpected because Belmont is maintained as a commercial lot while the orchard in Bible Hill is not. The range of nitrogen concentrations is relatively large, which will be helpful in creating comprehensive models. Soil nitrogen ranges from 1.23 – 24.54 ppm while needle tissue nitrogen ranges from 0.83 – 2.32%.

Normalized difference vegetation indices (NDVI) were created from multispectral camera photos and compared to soil and tissue nutrition. There were generally weak relationships between soil nutrition and NDVI, but there were stronger relationships between tissue N, P, and K and NDVI. The tissue nutrition relationships were even stronger for trees more than 5 years old. In particular, NDVI explained up to 60% of the variability in tissue N making it a decent predictive tool in determining N concentration in balsam fir.

LIST OF PUBLICATIONS

Nothing has been published to date, but one manuscript is being prepared:

MacDonald MT, Esau T, Bilodeau M. 2023. Effectiveness of normalized differences vegetation index in predicting tissue nutrition of young and mature balsam fir trees. Forests. Expected submission date September 2023.

FINANCIAL EXPENDITURE REPORT

Expense Category	Cost	Details
Personnel	$2000	One student was hired for this research. NSERC provided $6000 to cover their salary and the $2000 from CTPB covered the remainder.
Travel	$500	Fuel and per diem amounts for travel to 3 sites once in autumn and again in spring.
Equipment	$1000	User fee for the multispectral UAV and associated software.
Other	$6000	125 soil samples @ $19.05 mineral profile 125 soil samples @ $8.94 total nitrogen 125 tissue samples @ $20.65 mineral profile = $6080.00 * This slightly exceeded the budgeted amount, but excess was paid via another account. The original $6000 was listed in the “cost” column
Total	$9500	

Additional photos related to research

Figure 5. Orthomosaic image balsam fir orchard on Belmont Road, Belmont, NS.

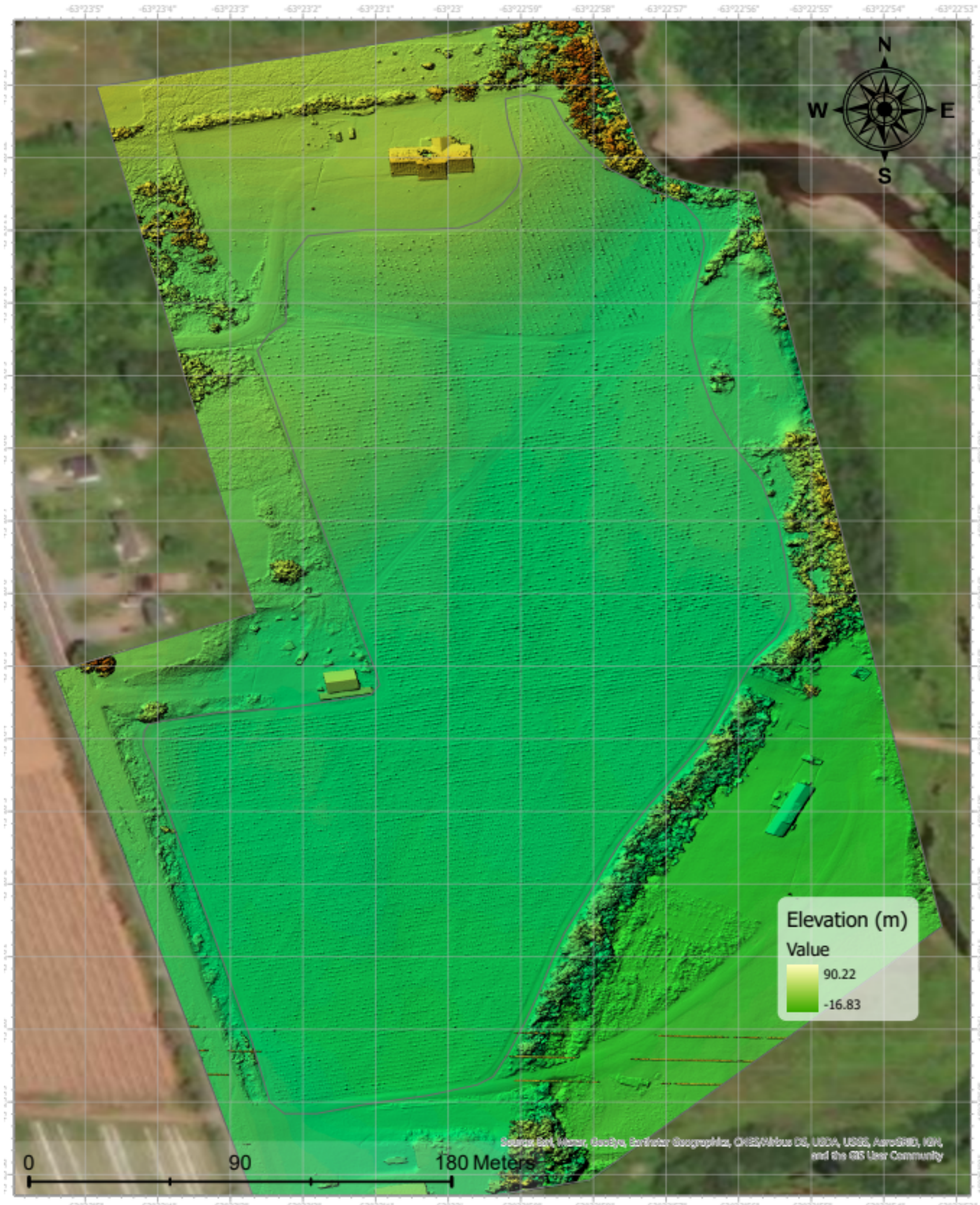

Figure 6. Digital elevation model of balsam fir orchard on Belmont Road, NS.

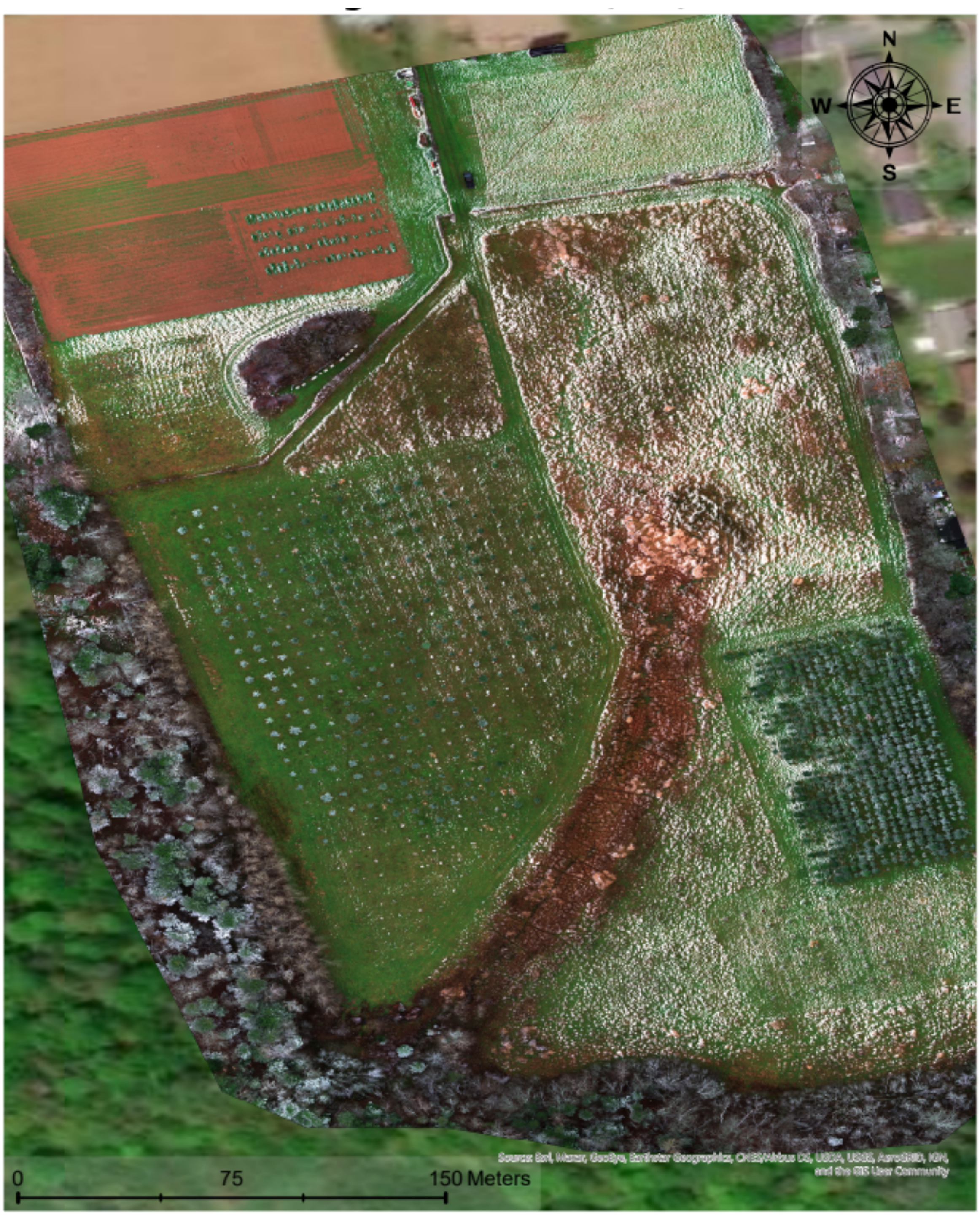

Figure 7. Orthomosaic image of balsam fir orchard on College Road, Bible hill, NS.

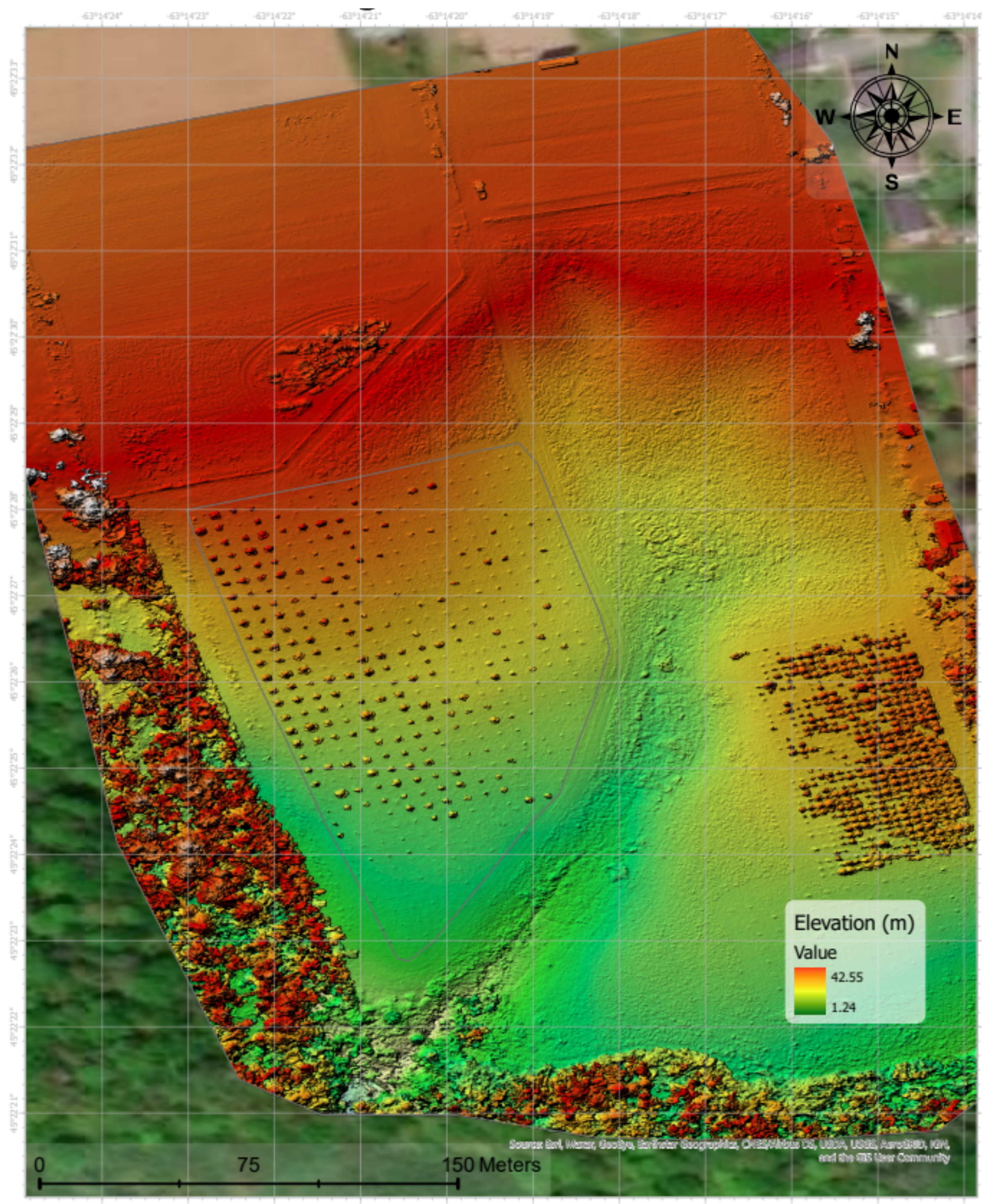

Figure 8. Digital elevation model of balsam fir orchard on College Road, Bible Hill, NS.